Size and surface orientation effects on thermal expansion coefficient of one-dimensional silicon nanostructures

H. Zhao and N. R. Aluru[a)]
Department of Mechanical Science and Engineering, Beckman Institute for Advanced Science and Technology, University of Illinois at Urbana-Champaign, Urbana, Illinois 61801, USA

(Received 18 August 2008; accepted 4 April 2009; published online 21 May 2009)

We perform classical molecular dynamics simulations based on the Tersoff interatomic potential to investigate the size and surface orientation dependence of lattice constant and thermal expansion coefficient of one-dimensional silicon nanostructures. Three different surface orientations of silicon are considered, i.e., Si(110), Si(111), and Si(100) with 2×1 reconstruction. For each surface orientation, we investigate nanostructures with thicknesses ranging from 0.3 to 5.0 nm. We compute the vibrational amplitude of surface atoms, lattice constant, and thermal expansion coefficient as a function of size and temperature, and compare them for different surface orientations. An analytical expression is developed to compute the variation of the thermal expansion coefficient with size of the nanostructure. © *2009 American Institute of Physics*. [DOI: 10.1063/1.3126499]

I. INTRODUCTION

Applications based on micro- and nanoelectromechanical systems (MEMS and NEMS) have grown substantially over the past few years. An important issue when dealing with micro- and nanoscale devices is to accurately predict their material properties as these properties can be different from macroscale devices. Both thermal and mechanical properties of a material can vary with the size of the nanostructure as finite size can break the symmetry of the crystal lattice. In recent years, several studies have been performed to predict the thermal and mechanical properties of perfect crystal lattices, e.g., silicon under various conditions such as temperature,[1] deformation,[2,3] etc. In order to accurately predict the material properties of nanostructures, systematic investigation of the variation of material properties with size and various surface orientations is important. Thermal amplitudes of silicon surface atoms with different surface orientations have been studied to show the anisotropic properties of vibrational amplitudes along different directions.[4] An *ab initio* study of silicon thin films has shown that the mechanical properties vary with the film thickness.[5] Using the local harmonic model, an augmented continuum theory has been proposed for the size dependence of the coefficient of thermal expansion of nanostructures.[6] However, for silicon, the local harmonic model may not accurately predict the variation of the lattice constant with temperature.[2] Since silicon is one of the important materials that is currently being investigated for MEMS/NEMS applications, a systematic investigation of the size and surface orientation effects in silicon is important.

Several theoretical methods and techniques have been developed to investigate material properties at the nanometer scale. *Ab initio* method[7] is one of the accurate techniques to predict the material properties, but it is also limited in use because of the large computational cost. With the development of empirical interatomic potentials,[8,9] which can be a reasonably accurate description of the material if the potentials are well-calibrated, methods such as lattice dynamics[10] or molecular dynamics (MD) can also be used to compute properties of nanoscale materials. Lattice dynamics methods are typically employed with a harmonic approximation of the potential and this can be an issue when the anharmonicity of the potential is important. MD simulations based on interatomic potentials can capture the anharmonicity and are much faster compared to the *ab initio* method. In this paper, we use MD simulation to investigate both the surface vibrational properties and the thermal expansion coefficient (TEC) of finite thickness silicon slabs (one-dimensional nanostructures) with three surface orientations at different temperatures. By investigating different slab thicknesses, we observe that the vibrational amplitude of the surface atoms remains constant when the silicon slab thickness is over 1.0 nm. The TEC of the interior of the slab, excluding the surface regions, is independent of the slab thickness if the slab thickness is over 1.0 nm. For slab thicknesses less than 1.0 nm, which corresponds to typically less than eight layers of silicon atoms, the TEC can be quite sensitive to both the thickness and the surface orientation. These observations could be useful for silicon-based NEMS applications.

The rest of the paper is organized as follows: in Sec. II, we introduce the nanostructures simulated and the MD simulation setup. Section III will present results on the vibrational amplitude of surface atoms. Section IV will discuss the lattice constant and interlayer relaxation of silicon at different temperatures. Section V will discuss the size dependence of the TEC of silicon slabs. Finally, conclusions are presented in Sec. VI.

II. SIMULATION DETAILS

Classical MD simulations are performed with the open source code LAMMPS.[11] To describe the interactions between silicon atoms, we use the Tersoff interatomic potential,[9] which has been used to predict structural properties of bulk

[a)]Author to whom correspondence should be addressed. Electronic mail: aluru@illinois.edu. URL: http://www.illinois.edu/~aluru.

0021-8979/2009/105(10)/104309/6/$25.00 © 2009 American Institute of Physics

Downloaded 21 May 2009 to 130.126.121.152. Redistribution subject to AIP license or copyright; see http://jap.aip.org/jap/copyright.jsp

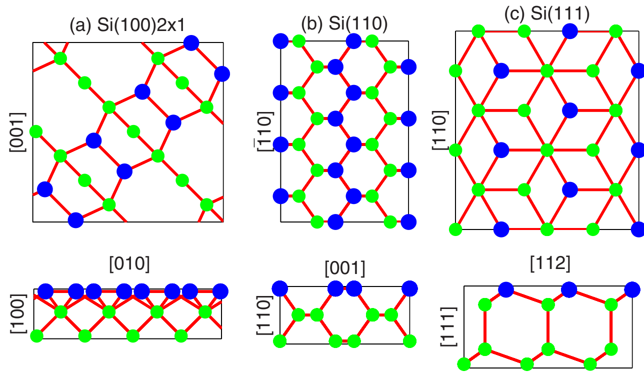

FIG. 1. (Color online) Top and side views of atomic positions of Si surfaces: (a) Si(100)2×1, (b) Si(110), and (c) Si(111). The big dark symbols represent the surface atoms. The small light symbols represent the atoms near the surface in the slab.

silicon,[1] silicon surfaces,[12] and silicon defects.[13] To investigate the dependence of thermal properties on size along a particular direction (e.g., the thickness direction), we model the infinite silicon slab by applying the periodic boundary condition along the two in-plane directions. To eliminate periodicity along the thickness direction, a vacuum space of 3.0 nm is added on either side of the surface. Nosé–Hoover thermostat[14] is employed to control the temperature with the *NPT* ensemble. A time step of 1.0 fs is used. All the simulations were run for 2.0 ns with the first 0.3 ns used for the system to reach an equilibrium state. Since classical MD simulations cannot capture quantum effects, which are important at low temperature, we employ the temperature rescaling method[15] to account for quantum corrections.

Three different structures with various low-index surfaces are constructed: Si(100), Si(110), and Si(111). With Tersoff potential, for the ideal Si(110) and Si(111) surfaces, the surface structure remains stable between the temperature range of 0–1500 K. The ideal Si(100) surface is not stable when the temperature is higher than 200 K and the symmetric 2×1 reconstructed structure is automatically formed. In this paper, we use the symmetric 2×1 reconstructed surface for the Si(100) structure instead of the ideal Si(100) surface. The top view and the side view of the three different orientations near the surface are shown in Fig. 1. The big dark symbols in the figures represent the surface atoms and the small light symbols represent the neighbors in the slab. We can observe from the figure that regardless of the surface orientation, every surface atom has three neighbor atoms with one dangling bond left free. When hydrogen passivation of the surface is considered with the Si–H interatomic potential,[16] the results indicate that the influence of hydrogen passivation on the thermal relaxation of silicon atoms can be negligible. In addition, with hydrogen passivation, the time step in MD simulations needs to be very small in order to maintain the Si–H bond. In this study, we consider the silicon surface without hydrogen passivation.

The initial configuration of the various structures in MD simulations are generated with the lattice constant a_0 =5.432 Å. Table I lists the dimensions of all the structures simulated. The in-plane size of the three structures is large enough to approximate the infinite in-plane with periodic

TABLE I. Dimensions (in nanometer) of different silicon structures considered.

	Si(100)2×1	Si(110)	Si(111)
In-plane dimensions	2.137×2.137	2.497×3.123	2.549×2.880
Thickness (number of layers)	0.367 (4)	0.384 (3)	0.392 (4)
	0.639 (6)	0.576 (4)	0.705 (6)
	0.911 (8)	0.768 (5)	1.646(12)
	1.454(12)	1.921(11)	2.586(18)
	1.997(16)	2.689(15)	3.527(24)
	3.084(24)	3.841(21)	
	4.170(32)	4.993(27)	

boundary conditions. For each surface orientation, we simulate five to seven different slab thicknesses ranging between 0.3 and 5.0 nm. All atoms having the same coordinate along the thickness direction are referred to as one layer of atoms. In Table I, the numbers in the parenthesis refer to the number of atom layers along the thickness direction of each structure.

III. VIBRATION AMPLITUDES

In experiments, vibrational properties of surface atoms can be studied with different techniques, such as He-atom scattering, surface infrared spectroscopy, etc. Thermal fluctuations of surface atoms play an important role in the dynamical processes of surface atoms. The root mean square vibrational amplitude (rmsVA) $\langle u_\alpha^2\rangle^{1/2}$, about the equilibrium position of a surface layer, is computed as

$$\langle u_\alpha^2\rangle^{1/2} = \left[\frac{1}{n_s}\sum_{i=1}^{n_s}\langle[r_{\alpha,i}(t) - \langle r_{\alpha,i}(t)\rangle]^2\rangle\right]^{1/2}, \tag{1}$$

where $\alpha=x,y,z$ denotes the spatial direction, n_s is the number of atoms on the surface layer, $r_{\alpha,i}(t)$ are the time (t) dependent coordinates of atom i in α direction, and $\langle\cdot\rangle$ denotes the time average.

The variation of rmsVA with temperature for Si(110), Si(111), and Si(100)2×1 surface atoms is shown in Fig. 2. The variation of rmsVA with temperature for bulk silicon atoms is also shown in the figure for comparison. Regardless of the orientation, the rmsVA of surface atoms increases faster with temperature compared to the rmsVA of a bulk atom. For the surface atoms, the out-of-plane rmsVA shows the strongest temperature dependence among all the three directions. The anisotropy between out-of-plane and in-plane rmsVA grows quickly with temperature. The magnitude of rmsVA for Si(100)2×1 surface matches with the results obtained from tight-binding calculations.[4] Of the three surfaces, Si(111) surface has the largest anisotropy between the out-of-plane and in-plane vibrations. Moreover, the rmsVA of surface atoms in the thickness direction of the Si(111) surface has the highest magnitude. This is because the Si(111) surface has the lowest surface atom density, which implies that the vibration of loosely packed surface atoms has larger amplitude. In the in-plane directions, since both Si(111) and Si(100)2×1 surfaces have uniform atom densities, the rmsVAs of surface atoms along these two directions are similar.

Downloaded 21 May 2009 to 130.126.121.152. Redistribution subject to AIP license or copyright; see http://jap.aip.org/jap/copyright.jsp

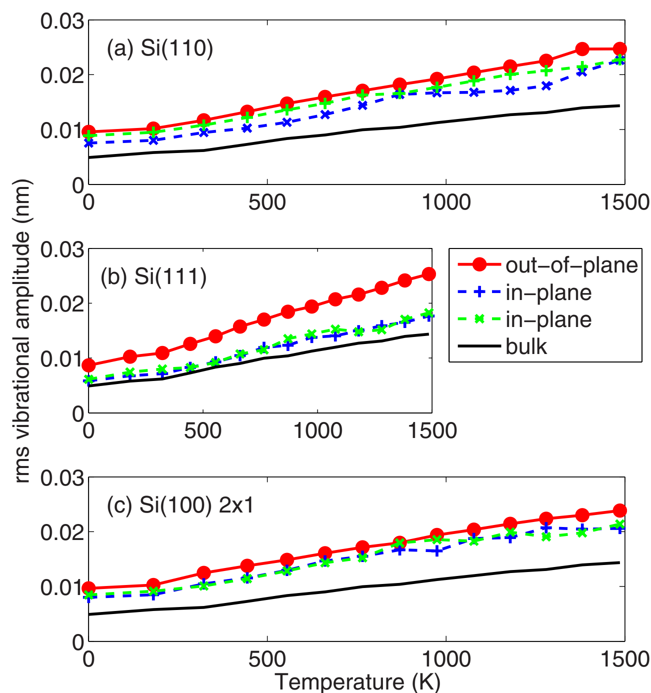

FIG. 2. (Color online) Variation of rmsVA of surface atoms with temperature for (a) Si(110), (b) Si(111), and (c) Si(100)2×1. The rmsVA for a bulk silicon atom is also shown for comparison.

However, for Si(110) surface, since the surface atoms are more densely packed in the $[\bar{1}10]$-direction than in the [001]-direction [see Fig. 1(b)], the rmsVAs along these two directions are different.

The variation of rmsVA in the out-of-plane direction as a function of temperature for different slab thicknesses of Si(110), Si(111), and Si(100)2×1 is shown in Fig. 3. For slab thickness over 1.0 nm, the variation of rmsVA with temperature is independent of slab thickness for all the three different surface orientations. However, for thicknesses below 1.0 nm, the thinner is the slab thickness, the higher is the magnitude of rmsVA, regardless of the surface orientation. When the slab thickness becomes quite small, the flatness and lattice structure of the silicon slab may not be maintained. For example, Fig. 4(a) shows the initial lattice structure of a 0.384 nm thick slab with Si(110) surface at 1000 K. Figure 4(b) shows a snapshot of the same slab when the structure attains the full relaxation state. We note that the structure is no longer flat and exhibits some bending. Similarly, Fig. 4(c) shows the initial lattice structure of a 0.367 nm thick slab with Si(100)2×1 surface at 1000 K. Figure 4(d) shows a snapshot of the same structure after the system has attained the equilibrium state. We again observe that the shape and structure of the lattice have been totally reconstructed and the initial atomic configuration is no longer maintained.

IV. LATTICE CONSTANT

In order to investigate the size dependence of thermal properties such as lattice constant and thermal expansion coefficient, for each surface orientation, we performed MD simulations with different slab thicknesses for temperatures between 0 and 1500 K. For a bulk system at equilibrium, the lattice constant is identical in all the three directions. However, for a finite thickness structure, since the two surfaces on the top and bottom of the slab break the symmetry of the lattice structure along the thickness direction, the relaxed interlayer spacings are no longer homogeneous. For a finite thickness structure at equilibrium, the lattice constant along the thickness direction can vary with location. Table II lists the average lattice constants of silicon slabs of various thick-

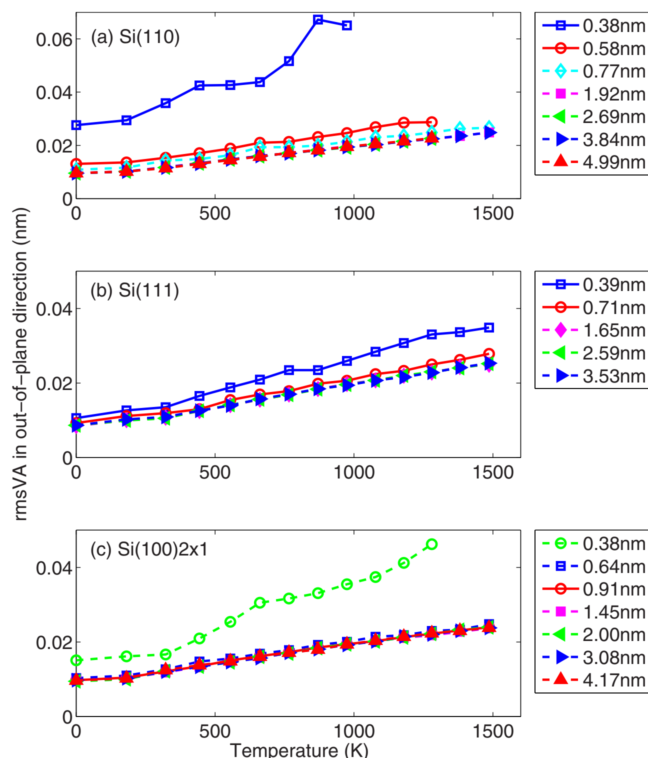

FIG. 3. (Color online) Variation of rmsVA of surface atoms with temperature in the out-of-plane direction for various slab thicknesses of (a) Si(110), (b) Si(111), and (c) Si(100)2×1.

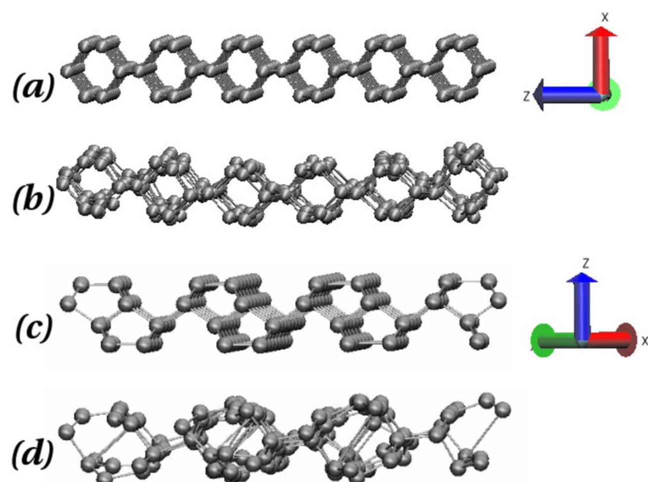

FIG. 4. (Color online) (a) Initial snapshot of a 0.384 nm thick slab with Si(110) surface at $T=1000$ K. (b) Snapshot of equilibrium configuration of a 0.384 nm thick slab with Si(110) surface at $T=1000$ K. (c) Initial snapshot of a 0.367 nm thick slab with Si(100)2×1 surface at $T=1000$ K. (d) Snapshot of equilibrium configuration of a 0.367 nm thick slab with Si(100)2×1 surface at $T=1000$ K.

Downloaded 21 May 2009 to 130.126.121.152. Redistribution subject to AIP license or copyright; see http://jap.aip.org/jap/copyright.jsp

TABLE II. Average lattice constant (in angstrom) of silicon for different surface orientations at various temperatures.

Si(110)								
Thickness (Å)	3.84	5.76	7.68	19.21	26.89	38.41	49.93	Bulk
300 K	4.973	5.173	5.247	5.372	5.394	5.410	5.418	5.446
600 K	4.965	5.177	5.253	5.380	5.402	5.419	5.427	5.455
900 K		5.181	5.259	5.389	5.412	5.429	5.437	5.466
Si(111)								
Thickness (Å)	3.92	7.05	16.46	25.86	35.27			Bulk
300 K	4.859	5.135	5.316	5.364	5.385			5.446
600 K	4.855	5.139	5.323	5.372	5.394			5.455
900 K	4.849	5.143	5.331	5.380	5.403			5.466
Si(100)2×1								
Thickness (Å)	3.67	6.39	9.11	14.54	19.97	30.84	41.70	Bulk
300 K	5.183	5.347	5.382	5.411	5.422	5.430	5.435	5.446
600 K		5.353	5.387	5.417	5.429	5.438	5.443	5.455
900 K		5.364	5.393	5.425	5.438	5.448	5.453	5.466

nesses with three different surface orientations when the temperature equals 300, 600, and 900 K. As the slab thickness increases, the average lattice constant increases and converges to the bulk value. For a given slab thickness, as the temperature increases, the average lattice constant increases.

In order to clearly understand how the atom locations vary along the thickness direction of a finite thickness slab, we compute the interlayer distance, which is defined as

$$d_{i,i+1} = \frac{1}{n_{i+1}} \sum_{j \in n_{i+1}} r_{\alpha,j} - \frac{1}{n_i} \sum_{j \in n_i} r_{\alpha,j}, \tag{2}$$

where n_i and n_{i+1} are the number of atoms on layer i and layer $i+1$, respectively. $r_{\alpha,j}$ is the coordinate of atom j along the thickness direction α and $d_{i,i+1}$ is the interlayer distance between layer i and $i+1$. Using the 4.993 nm thick silicon slab with Si(110) surface as an example, Fig. 5 shows the variation of interlayer distance for different temperatures. The interlayer distance of the surface atoms is much smaller compared to the interlayer distance of inside atoms because of the asymmetry of bond forces on the surface atoms. Furthermore, since silicon is a diamond structure, the asymmetry of the surface structure influences the interlayer distance of the first four layers of atoms near the surface. Inside the slab, the interlayer distance does not change. The interlayer distance increases with temperature. However, the increase in interlayer distance with temperature for surface atoms is smaller compared to that of the atoms inside the slab. We observed similar results with Si(100)2×1 and Si(111) surfaces.

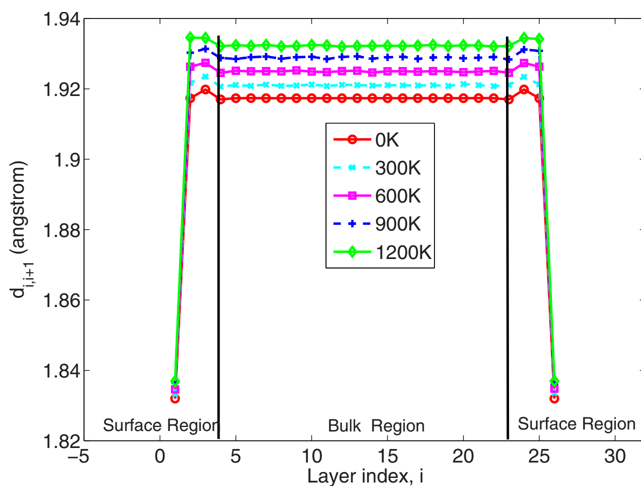

FIG. 5. (Color online) Si(110) interlayer distance for various temperatures.

V. TEC

Thermal expansion is the tendency of matter to change in volume in response to a change in temperature. Linear TEC $\alpha(T)$ is a function of temperature T and can be defined as

$$\alpha(T) = \frac{1}{l_0} \frac{\partial l(T)}{\partial T}, \tag{3}$$

where $l(T)$ is the length of the system at temperature T and l_0 is the length of the system at temperature $T=T_0$. Here we use $T_0=0$ K. For conciseness, in the following, we express $\alpha(T)$ and $l(T)$ as α and l.

To investigate how the structure expands with temperature along the finite thickness direction, when the slab thickness is larger than 1.0 nm, the structure is decomposed into two surface regions and one bulk region, as shown in Fig. 5. Thus, we can define the thickness of the silicon slab l as the sum of the surface region thickness l_s and the bulk region thickness l_b, i.e.,

$$l = 2l_s + l_b = 2\rho d_s + h d_b, \tag{4}$$

where d_s and d_b are the average interlayer distances in surface and bulk regions, respectively. ρ is a parameter that defines the number of layers in the surface region and h defines the number of layers in the bulk region of the slab. For Si(111) surface orientation, since the interlayer distance alternates between two values d_1 and d_2, we define the inter-

Downloaded 21 May 2009 to 130.126.121.152. Redistribution subject to AIP license or copyright; see http://jap.aip.org/jap/copyright.jsp

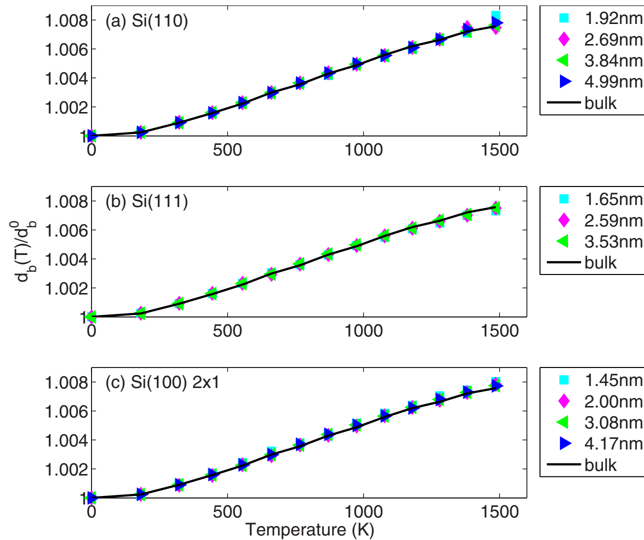

FIG. 6. (Color online) Variation of the normalized average interlayer distance with temperature for the bulk region of silicon slabs of various thicknesses of (a) Si(110), (b) Si(111), and (c) Si(100)2×1 surface orientations.

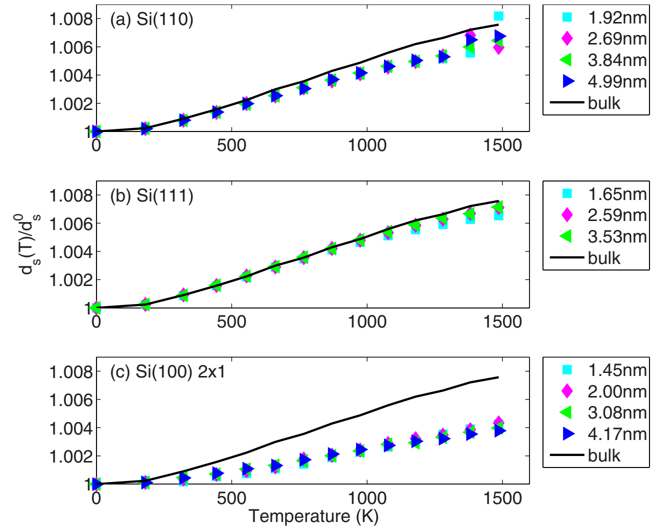

FIG. 7. (Color online) Variation of the normalized average interlayer distance with temperature for the surface region of silicon slabs of various thicknesses of (a) Si(110), (b) Si(111), and (c) Si(100)2×1 surface orientations.

layer distance as $d=d_1+d_2$ for both the surface and the bulk regions. For Si(110), Si(111), and Si(100)2×1 surface orientations, the value of ρ is 3, 2, and 2.8544, respectively. Substituting Eq. (4) into Eq. (3), we obtain

$$\alpha = \frac{1}{l_0}\left(2\frac{\partial l_s}{\partial T} + \frac{\partial l_b}{\partial T}\right). \tag{5}$$

For the surface and bulk regions of the structure, the thermal expansion coefficients α_s and α_b can be defined as

$$\alpha_s = \frac{1}{l_s^0}\frac{\partial l_s}{\partial T} = \frac{1}{d_s^0}\frac{\partial d_s}{\partial T}, \quad \alpha_b = \frac{1}{l_b^0}\frac{\partial l_b}{\partial T} = \frac{1}{d_b^0}\frac{\partial d_b}{\partial T}, \tag{6}$$

where l_s^0, l_b^0, d_s^0, and d_b^0 are the lengths of the surface region, bulk region, the average interlayer distance of the surface region and the bulk region, respectively, at temperature T_0. Figures 6 and 7 show the variation of the normalized average interlayer distance with temperature for both the bulk and the surface regions when the slab thickness is over 1.0 nm. We found that the TEC (slope of the curve) is independent of the size of the slab, for both the bulk and the surface regions. The normalized lattice constant of the bulk region matches with the normalized lattice constant of bulk silicon. For the surface region, the variation of the normalized lattice constant with temperature deviates from that of the bulk. By fitting a fifth-order polynomial to the data shown in Figs. 6 and 7, we compute the thermal expansion coefficients α_s and α_b by using Eq. (6). The variation of α_s and α_b with temperature for different surface orientations is shown in Fig. 8. The TEC of the bulk region is independent of both the size and the surface orientation of the structure. However, α_s varies with the surface orientations. Substituting Eq. (6) into Eq. (5), we obtain the relationship between α, α_b, and α_s as

$$\frac{\alpha - \alpha_b}{\alpha_b} = \frac{\dfrac{\alpha_s}{\alpha_b} - 1}{1 + \dfrac{h d_b^0}{2\rho d_s^0}}. \tag{7}$$

We define $K=d_b^0/d_s^0$ as the ratio of average interlayer distance of bulk region to the surface region of the structure at T_0. Figure 9 shows the variation of K with the slab thickness for the three different surface orientations. We observe that for each surface orientation, the variation of K with thickness is negligible, implying that K is almost independent of the slab thickness. Moreover, from Fig. 9, for Si(110), Si(111), and Si(100)2×1 surface orientations, the value of K is 1.0152, 1.0057, and 1.0528, respectively. Since the variation of K with respect to the surface orientations is quite small

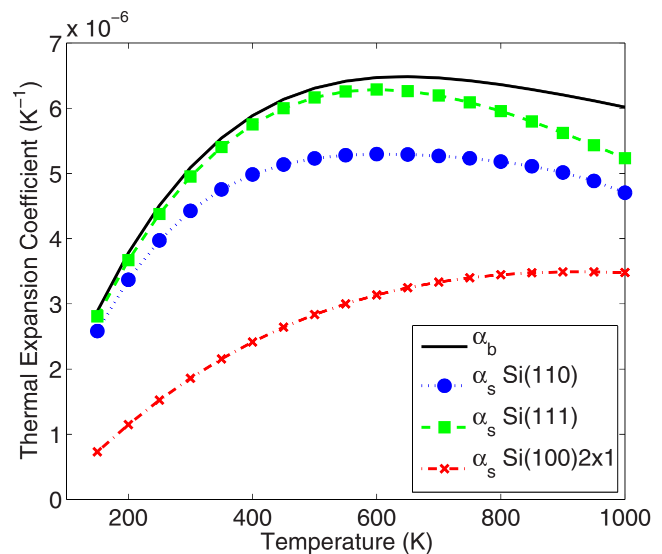

FIG. 8. (Color online) Thermal expansion coefficients, α_b and α_s, for slab thicknesses over 1.0 nm.

Downloaded 21 May 2009 to 130.126.121.152. Redistribution subject to AIP license or copyright; see http://jap.aip.org/jap/copyright.jsp

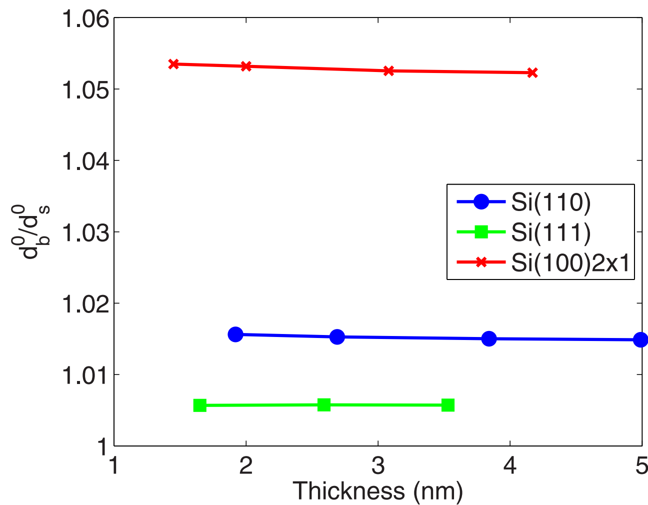

FIG. 9. (Color online) Variation of $K=d_b^0/d_s^0$ with slab thickness.

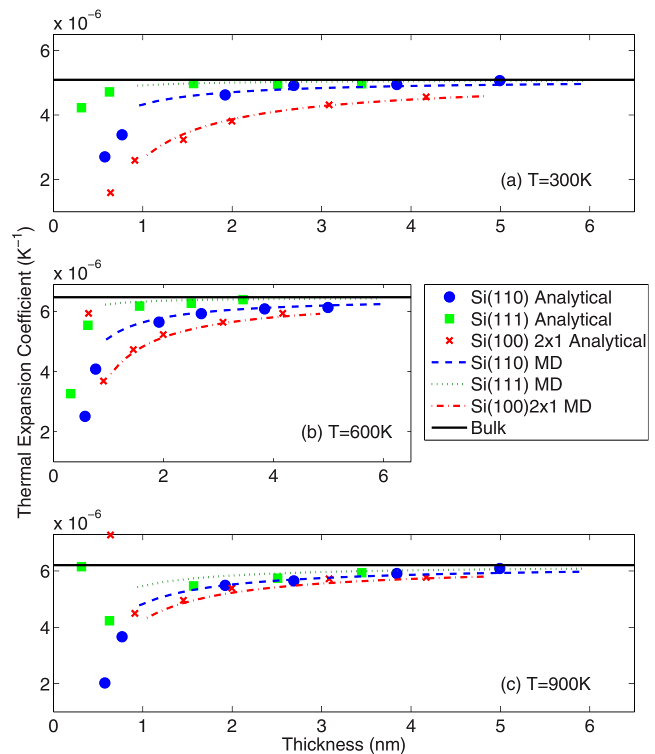

FIG. 10. (Color online) Variation of the TEC with slab thickness for different surface orientations at (a) $T=300$ K, (b) $T=600$ K, and (c) $T=900$ K.

and close to 1.0, for simplicity, we just assume $K=1.0$ in the derivation of the analytical expression.

Equation (7) can be rewritten as

$$\alpha = \frac{2\rho\alpha_s + h\alpha_b}{2\rho + h} = (1-t)\alpha_s + t\alpha_b, \tag{8}$$

where $t=h/(2\rho+h)$ is the ratio of the thickness of the bulk region to the total thickness of the structure. For each specified temperature, once α_b and α_s are calculated, the variation of the TEC with the size of the structure can be predicted using Eq. (8). Figure 10 shows the comparison between the TEC obtained from MD and analytical approach [Eq. (8)] at $T=300$ K, $T=600$ K, and $T=900$ K for the different surface orientations. Note that the analytical expression is used only for slab thicknesses larger than 1.0 nm. As shown in Fig. 10, for larger than 1.0 nm slab thicknesses, the TEC of silicon slab increases with thickness and converges to the bulk value, regardless of the surface orientation. We note that the results from the analytical expression [Eq. (8)] compare well with MD data, as shown in Fig. 10. For slab thicknesses less than 1.0 nm, the TEC can be quite sensitive to both the surface orientation and the slab thickness.

VI. CONCLUSIONS

In this paper, we investigated the size and surface orientation dependence of thermal properties by using classical MD simulations based on the Tersoff interatomic potential. We found that regardless of the surface orientation, the variation of the surface rmsVA with temperature is independent of the slab thickness when the thickness is over 1.0 nm. The surface TEC and the bulk TEC are also independent of the slab thickness. When the thickness is over 1.0 nm, the surface TEC varies with the surface orientation, while there is no such dependence on the bulk thermal expansion coefficient. When the slab thickness is less than 1.0 nm, both the rmsVA and TEC of the structure along the thickness direction can strongly depend on the surface orientation and thickness. Finally, we also developed an analytical expression for the variation of TEC with size and we show that the results from the analytical expression match well with MD results.

ACKNOWLEDGMENTS

We gratefully acknowledge support by the National Science Foundation under Grant Nos. 0519920, 0601479, and 0810294.

[1]L. J. Porter, S. Yip, M. Yamaguchi, H. Kaburaki, and M. Tang, J. Appl. Phys. **81**, 96 (1997).
[2]H. Zhao, Z. Tang, G. Li, and N. R. Aluru, J. Appl. Phys. **99**, 064314 (2006).
[3]Z. Tang, H. Zhao, G. Li, and N. R. Aluru, Phys. Rev. B **74**, 064110 (2006).
[4]O. L. Alerhand, J. D. Joannopoulos, and E. J. Mele, Phys. Rev. B **39**, 12622 (1989).
[5]Y. Umeno, A. Kushima, T. Kitamura, P. Gumbsch, and J. Li, Phys. Rev. B **72**, 165431 (2005).
[6]S. Pathak and V. B. Shenoy, Phys. Rev. B **72**, 113404 (2005).
[7]S. Wei, C. Li, and M. Y. Chou, Phys. Rev. B **50**, 14587 (1994).
[8]F. H. Stillinger and T. A. Weber, Phys. Rev. B **31**, 5262 (1985).
[9]J. Tersoff, Phys. Rev. B **38**, 9902 (1988).
[10]R. LeSar, R. Najafabadi, and D. J. Srolovitz, Phys. Rev. Lett. **63**, 624 (1989).
[11]S. J. Plimpton, J. Comput. Phys. **117**, 1 (1995).
[12]H. Balamane, T. Halicioglu, and W. A. Tiller, Phys. Rev. B **46**, 2250 (1992).
[13]A. Yu. Belov, K. Scheerschmidt, and U. Gsele, Phys. Status Solidi A **171**, 159 (1999).
[14]W. G. Hoover, Phys. Rev. A **31**, 1695 (1985).
[15]C. Z. Wang, C. T. Chan, and K. M. Ho, Phys. Rev. B **42**, 11276 (1990).
[16]U. Hansen and P. Vogl, Phys. Rev. B **57**, 13295 (1998).

Downloaded 21 May 2009 to 130.126.121.152. Redistribution subject to AIP license or copyright; see http://jap.aip.org/jap/copyright.jsp